Chemical Engineering Science 144 (2016) 58–74

Contents lists available at ScienceDirect

Chemical Engineering Science

journal homepage: www.elsevier.com/locate/ces

Characterizing bubble column bioreactor performance using computational fluid dynamics

Dale D. McClure [a], John M. Kavanagh [a], David F. Fletcher [a,*], Geoffrey W. Barton [a]

[a] School of Chemical and Biomolecular Engineering, The University of Sydney, NSW 2006, Australia

HIGHLIGHTS

- Kinetics of microbial growth implemented in CFD model.
- Lagrangian particle tracking used to quantify impact of reactor design.
- A range of metrics were used to quantify impact of bioreactor design on performance.
- Impact of substrate addition point on yield examined.
- Approach developed can be used for design and optimisation of bioreactors.

GRAPHICAL ABSTRACT

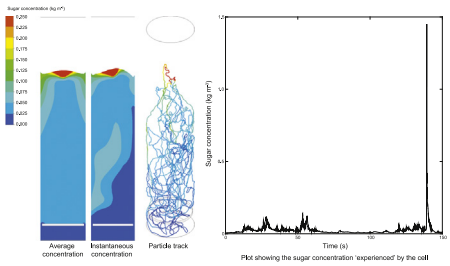

ARTICLE INFO

Article history:
Received 21 April 2015
Received in revised form
11 December 2015
Accepted 1 January 2016
Available online 22 January 2016

Keywords:
Bubble column
CFD
Bioreactors
Bioprocess
Scale-up

ABSTRACT

In this work we have coupled microbial kinetics with a Computational Fluid Dynamics (CFD) model of the hydrodynamics within a bubble column. *Saccharomyces cerevisiae* was used as a model organism due to its well characterized kinetics. A range of methodologies was used to quantify the impact of reactor design on performance. These methodologies included those based on the average substrate concentration, those based on the instantaneous substrate concentration, as well as those based on Lagrangian particle tracking. By using the particle tracking approach it was possible to quantify the duration of any oscillations in substrate concentration that the cells experience, a question of key physiological relevance. It was found that the relative yield as calculated using both approaches depended on the sugar addition location. Values of the relative yield between 75% and 93% were calculated based on the average concentration approach, 73–81% based on the instantaneous concentration approach; while values of 93–97% were calculated using particle tracking. Overall, the results from this work clearly demonstrate the potential of using CFD to characterize the complex and highly dynamic behaviour occurring in bubble column bioreactors.

1. Introduction

Bubble columns are gas-liquid contactors which are widely used in the bio-processing industry to produce a range of products (Kantarci et al., 2005). A key consideration in any industrial bioprocess is maximising the yield (typically defined as the mass of product produced per mass of substrate added). It has been observed that as a process is scaled-up the yield decreases; the magnitude of this reduction has been reported to be 6–7% for the production of baker's yeast (*Saccharomyces cerevisiae*) (George et al., 1998) and approximately 20% for the production of recombinant protein using *Escherichia coli* (Enfors et al., 2001).

This difference in yield has been attributed to substrate gradients which are caused by poor mixing. Such gradients can lead to the cells being exposed to high substrate concentrations which can trigger overflow metabolism in many industrially relevant microorganisms. For example, in the case of *S. cerevisiae* production,

* Corresponding author. Tel.: +61 2 9351 4147.
E-mail address: david.fletcher@sydney.edu.au (D.F. Fletcher).

http://dx.doi.org/10.1016/j.ces.2016.01.016
0009-2509/

exposure to high sugar concentrations leads to the production of ethanol (the Crabtree effect), which in turn leads to a reduction in yield (George et al., 1998). Similar behaviour occurs with *E. coli* with acetate being the typical product of overflow metabolism (Xu et al., 1999). As noted elsewhere (Kavanagh and Barton, 2008), acetate can inhibit the production of recombinant protein; hence, it is desirable to avoid conditions which lead to acetate production.

Exposure to zones where the substrate concentration is very low may lead to starvation, which also negatively affects the yield. Additionally, it has been shown (Hewitt and Nienow, 2007) that exposure to fluctuating environmental conditions can induce the stress response in *E. coli*, which again results in a reduction in the yield.

A number of authors (Bylund et al., 1999; Sweere et al., 1988; Xu et al., 1999) have examined the impact of exposing cells to fluctuating conditions; work that has been reviewed by Lara et al. (2006) and Neubauer and Junne (2010). Such approaches provide insight into the problems associated with substrate gradients; however, they offer little insight as to how the design or operation of large-scale reactors can be improved so as to minimise yield loss.

In order to begin to address this industrially important issue, several authors (Morchain et al., 2014; Vetter, 2009; Vrábel et al., 2001) have examined coupling a Computational Fluid Dynamics (CFD) model with relevant microbial kinetics, with the aim of developing a meaningful model of bioprocesses.

A key difficulty in any bioprocess modelling is the need to account for a wide range of time-scales. For example a typical fed-batch fermentation for the production of *S. cerevisiae* is of the order 12–18 h (Vetter, 2009); while the maximum specific growth rate of yeast is around 0.5–0.6 h^{-1} (Blanch and Clark, 1997) (meaning that the cell concentration will double approximately every 70 min). Scale-down studies performed at the laboratory scale have shown that exposing yeast to fluctuating environmental conditions with circulation times of the order 30–60 s is sufficient to cause an increase in by-product formation, as well as a drop in biomass (Lara et al., 2006). In comparison, characteristic relaxation times for bubbles in two-phase flow are of the order 1×10^{-3} s (Braun, 2012). Simulating behaviour across such a range of time-scales (seven orders of magnitude) represents a significant challenge.

One possible method of addressing this issue has been used by Vetter (2009) where a CFD model is coupled with a separate model of biological growth. In this 'sequential co-simulation' approach, the flow-patterns predicted by the CFD model are used to calculate the local concentrations of all relevant species (e.g. oxygen, glucose, ethanol, etc.). This information is then used by the biological model to calculate the rates of growth and consumption, with the resultant information being returned to the CFD model. A major advantage of this approach is that it is possible to simulate the entirety of a fed-batch fermentation, something which is too computationally demanding if the growth kinetics are incorporated directly into the CFD model. The reason for this is that relatively small (of the order 1×10^{-3} s) time-steps are needed to simulate the fluid flow, while typical fermentations can be 12–18 h in duration. Vetter (2009) divided an 18 h fermentation into four increments, obtaining excellent agreement with his experimental results. It was also noted that computational efficiency was a key consideration in the simulation of industrial systems; such a conclusion having also been reached by others (Noorman, 2011).

An alternative approach has been used by Morchain et al. (2014) to model growth in a stirred-tank bioreactor. In their work, they have introduced a population balance model for the biomass to account for the different concentrations experienced by the cells. In this approach, the local specific growth rate is decoupled from the population specific growth rate, meaning that the impact of poor substrate distribution can be accounted for in the model. By calculating the difference between local and global specific growth rates, it is possible to identify zones where the cells are exposed to excess or insufficient substrate concentrations.

In their work Lapin et al. (2006) developed an Euler–Lagrange model of *E. coli* growth in a stirred tank where the movement of cells throughout the reactor is tracked. The key advantage of this approach is that it is possible to quantify the degree to which the cells are exposed to fluctuating environmental conditions, such knowledge being very useful in quantifying the effect of reactor design on performance (i.e. yield).

A range of methodologies exist by which the performance of a bioreactor can be quantified. Hence, the key aim of the present work is to build upon these existing approaches and examine their potential as tools for quantifying the impact of reactor design on performance. We will focus on examining a *S. cerevisiae* fermentation; for the reason that it is a commonly used microorganism with well characterized genetics and kinetics.

2. Model set-up

2.1. CFD set-up

Here we have extended an existing CFD model of bubble column hydrodynamics that has been validated against a comprehensive experimental data set including measurements of local hold-up profiles, profiles of the gas and liquid velocity, bubble size distribution and mixing time (as a function of tracer addition and measurement location) (McClure et al., 2014b, 2014c, 2015a).

The system modelled was a pilot-scale bubble column 0.39 m in diameter and 2 m in height as shown schematically in Fig. 1. Air was introduced through a 'tree' type sparger, the centerline of which is located at a height (z) of 0.135 m, at a superficial velocity of 0.16 m s^{-1}.

In order to quantify the impact of reactor design, substrate was introduced in three different ways. The first substrate addition location (injection point 1) was located at the column centerline at a height (z) of 1.5 m; this position being chosen as substrate addition at the free surface is commonly employed. Injection point 2 was positioned at the column centerline, 0.05 m above the base of the column (i.e. below the sparger), with this position being selected on the basis that this is the most poorly mixed region of the column (McClure et al., 2015a). Addition below the sparger is unlikely to be used in any practical set-up, however, this location was chosen as it was felt that it would provide an interesting point of comparison with the more commonly used approach (i.e. adding substrate at the free surface). Finally, sugar was introduced as a volume source uniformly throughout the column, such an approach corresponding to perfect mixing whereby the substrate introduced is instantaneously and uniformly dispersed throughout the column. In all cases, the sugar was introduced at the same rate ($S_{Feed} = 1.1 \times 10^{-3}$ kg s^{-1}). Concentrations (i.e. of sugar, cells, etc.) are calculated on the basis of the liquid-phase volume (and not the two-phase volume) as is physically correct. The three sugar tracers have been introduced as separate scalars, with the kinetics of uptake being calculated for each individual scalar. All of the scalars share the same flow field; hence any predicted differences in sugar concentration and product yield are only a function of the addition point.

The approach used to solve the fluid-flow inside the reactor will be described here briefly; a more detailed description (including the relevant equations) has been presented in Appendix A. Here, we have used the Euler–Euler approach to model the two-phase flow; with ANSYS CFX 15.0 being used to solve the

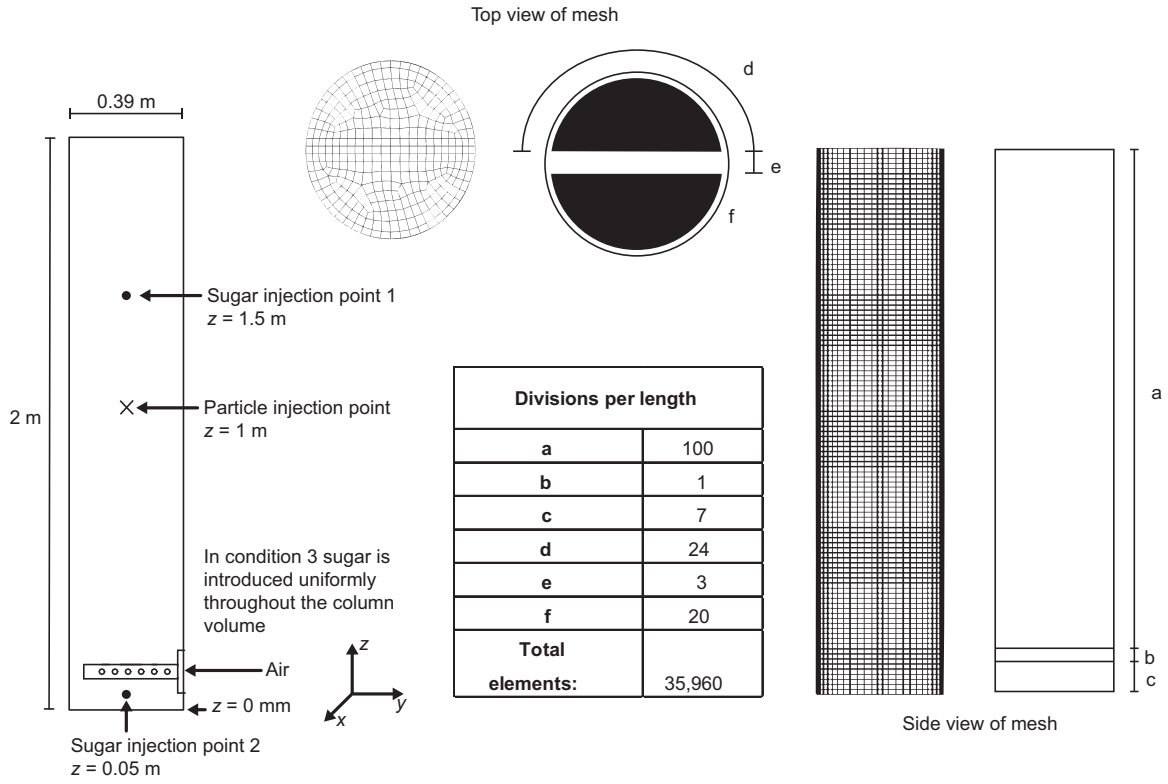

Divisions per length	
a	100
b	1
c	7
d	24
e	3
f	20
Total elements:	35,960

Fig. 1. Schematic showing CFD model set-up, including details about the mesh used.

equations. In our modelling approach, inter-phase momentum transfer is modelled using the Grace et al. (Clift et al., 1978) correlation to determine the drag force experienced by an isolated bubble, combined with a modified form of the volume fraction correction term developed by Simonnet et al. (2007) to account for the change in drag due to the presence of other bubbles. Additionally, as outlined elsewhere (McClure et al., 2015c), the drag law was modified to include an empirical parameter to account for the impact of surfactant addition, which is necessary to correctly describe systems with significant surfactant levels such as fermentation media. Turbulent dispersion was modelled using the Favre-averaged drag model (Burns et al., 2004). Turbulence in the liquid phase was modelled using the k–ε model which was modified to include the source terms developed by Pfleger and Becker (2001) to account for bubble-induced turbulence. Further details about the equations solved in the model are presented in Appendix A, as well as elsewhere in the literature (McClure et al., 2014b, 2014c).

Fig. 1 also illustrates the computational mesh used in this work. Prior to undertaking this study, a range of meshes was evaluated (McClure et al., 2014c); it was found that further refinements to the mesh did not lead to substantial differences in the model predictions.

The bubble column was modelled as a transient system, using the second-order backward Euler transient scheme; the high-resolution advection scheme was used for the convective terms. Fixed time steps of 1×10^{-3} s were used, with all simulations being performed using double precision.

A single bubble size of 5 mm was used in the model, corresponding to the experimentally measured mean size in fermentation media (McClure et al., 2013). The oxygen transfer rate (OTR) was calculated according to:

$$\mathrm{OTR} = k_L a\left(C^* - C\right) \tag{1}$$

where k_L is the liquid film mass transfer coefficient, a is the interfacial area for mass transfer, C^* is the saturation oxygen concentration and C is the dissolved oxygen concentration. An experimentally measured value of 2×10^{-4} m/s was used for k_L, this value being obtained for systems containing surfactants (McClure et al., 2015b). The interfacial area (a) was calculated according to:

$$a = \frac{6\alpha}{d_b} \tag{2}$$

where α is the volume fraction of the gas phase and d_b is the diameter of the bubble (5 mm).

C^* was calculated using Henry's law, using a value of 77,942 Pa m^3 mol^{-1} for Henry's law constant (Doran, 1995), such a value corresponding to a dissolved oxygen concentration of 8.5 mg/L at atmospheric pressure.

2.2. Kinetic modelling

Generally speaking the rate at which the sugar concentration (S) changes with time (t) due to sugar up-take by the cells depends on the concentration of cells (X), as well as the specific consumption rate (r_s):

$$\frac{dS}{dt} = -r_s X \tag{3}$$

The specific consumption rate depends on the local substrate concentration. Various authors (Auling et al., 1984; Pham et al., 1998; Postma et al., 1989; Sonnleitner and Käppeli, 1986) have proposed functions that relate substrate consumption rate to its concentration, which typically have the form of Monod kinetics:

$$r_S = \frac{r_{S,\max} S}{K_S + S} \tag{4}$$

where $r_{S,\max}$ is the maximum specific substrate uptake rate and K_S is the substrate saturation parameter. A comparison between these various models is presented in Fig. 2. In this work we used the

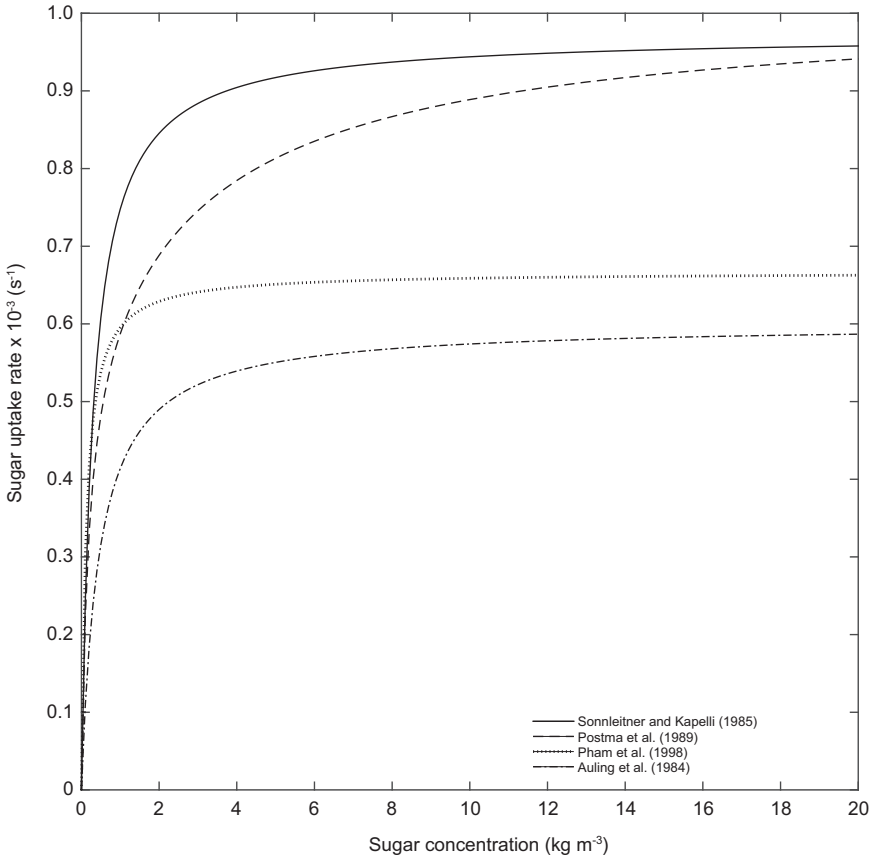

Fig. 2. Comparison between published (Auling et al., 1984; Pham et al., 1998; Postma et al., 1989; Sonnleitner and Käppeli, 1986) sugar uptake rates as a function of substrate (glucose) concentration.

Table 1
List of model parameters.

Parameter	Description	Value	Units
d_b	Bubble diameter	5	mm
H	Henry's Law constant for oxygen	77,942	Pa m^3 mol^{-1}
k_L	Liquid film mass transfer coefficient	2×10^{-4}	m/s
K_O	Oxygen saturation parameter	1×10^{-4}	kg m^{-3}
K_S	Substrate saturation parameter	0.3	kg m^{-3}
m_S	Maintenance coefficient	7.1×10^{-6}	s^{-1}
$r_{O,max}$	Maximum specific oxygen uptake rate	7.1×10^{-5}	s^{-1}
$r_{S,max}$	Maximum specific substrate uptake rate	9.7×10^{-4}	s^{-1}
$r_{S,aero,max}$	Maximum aerobic sugar consumption rate	1.7×10^{-4}	s^{-1}
S_{Feed}	Sugar feed rate	1.1×10^{-3}	kg s^{-1}
$Y_{aerobic}$	Biomass yield under aerobic conditions	0.49	–
$Y_{anaerobic}$	Biomass yield under anaerobic conditions	0.05	–
X	Cell concentration	50	kg m^{-3}

values of $r_{S,\max}$ and K_S suggested by Sonnleitner and Käppeli (1986), with a full listing of the parameters used being presented in Table 1.

As shown in Fig. 2, there is some difference in the predicted rate of substrate consumption and this may impact on the model predictions. Here we have chosen to use the model of Sonnleitner and Käppeli (1986) as this is a widely used model of aerobic yeast growth, and hence is a useful starting point in the evaluation of different modelling approaches. An interesting area of future research would be to examine different kinetics; either to include the sugar uptake expressions by different authors, or to examine the kinetics for a different microorganism.

As previously noted, exposure to high sugar concentrations may lead to overflow metabolism in many industrially important microorganisms, while exposure to low sugar concentrations may lead to starvation. Hence, it can be reasonably concluded that an optimum reactor design will be such that the cells are exposed to a homogeneous sugar concentration below the value where overflow metabolism will occur, but above the value where the cells will be starved. Therefore, it is essential to define the substrate concentrations which lead to these two undesirable conditions.

A reasonable estimate of the minimum sugar uptake rate necessary to avoid starvation may be provided by the maintenance coefficient (m_S), which defines the rate of substrate consumption necessary to maintain cellular processes without any cell growth. Values of the maintenance coefficient for baker's yeast are of the order 5×10^{-6} kg glucose per kilogram of dry cell mass per second (Blanch and Clark, 1997). If cells are exposed to local sugar concentrations below this value, they can be considered as starving, as they are not being supplied with sufficient substrate to meet their minimal requirements. It is certainly possible to devise alternative metrics to quantify the extent to which cells are not being supplied with sufficient substrate (Morchain et al., 2014), however, here we have chosen to use a relatively simple approach in order to best compare the range of metrics examined.

Identifying the sugar concentration which will lead to overflow metabolism is more contentious. Sonnleitner and Käppeli (1986) proposed that yeast have a limited respiratory capacity, with any excess sugar being 'diverted' to fermentative metabolism. They suggested that the value for the maximum rate at which substrate can be utilised aerobically ($r_{S,aero,\max}$) is of the order 1.7×10^{-4} kg per kilogram of dry cell mass per second. If the substrate concentration is such that the specific sugar uptake rate is greater

Table 2
Comparison of performance metrics evaluated in this work.

	Method	Advantages	Disadvantages
Concentration Based Methods	Calculate volume of reactor experiencing overflow metabolism. Eqs. (11) and (12).	Relatively simple method. Allows performance to be quantified as a function of design.	Does not account for transient behaviour.
	Calculate volume of reactor experiencing starvation. Eqs. (9) and (10).	Relatively simple method. Allows performance to be quantified as a function of design.	Does not account for transient behaviour.
	Calculate average relative yield. Eq. (13).	Relatively simple method. Metric is commercially relevant.	Does not account for transient behaviour.
	Calculate instantaneous relative yield. Eq. (13).	Relatively simple method. Metric is commercially relevant.	Does not account for duration of fluctuations.
Particle Tracking Methods	Generate plot of substrate concentration as a function of time for each particle. (e.g. Fig. 8).	Clearly illustrates transient behaviour.	Impractical for any reasonable number of particles.
	Calculate average yield for each particle Eqs. (15)–(17).	Captures transient behaviour. Commercially relevant metric.	Increased post-processing effort.
	Calculate frequency distribution of mean sugar concentration Eq. (14).	Gives an insight into how uniform the conditions seen by the cells are.	Averaging may favour high concentrations.
	Calculate amount of time spent in overflow or starvation conditions.	Summarizes transient behaviour.	Does not account for concentration.
	Calculate the number, length or frequency at which particles experience oscillations above the aerobic maximum or below the maintenance value.	Summarizes transient behaviour. Method can be used to give an insight into whether fluctuations occur at physiologically relevant timescales.	Increased post-processing effort.

than this value (i.e. $S > 0.063\ \mathrm{kg\ m^{-3}}$), it may be reasonably concluded that cells exposed to these conditions will undergo overflow metabolism. It is important to note that exposure to sugar concentrations above this aerobic maximum will induce overflow metabolism even if sufficient oxygen is present (the Crabtree effect) (Walker, 1998). Hence, the key consideration in baker's yeast production is to minimise areas within the bubble column where there is a high, local substrate concentration.

Despite this, it is important to supply the yeast with sufficient oxygen in order to favour aerobic metabolism. The concentration of dissolved oxygen depends on the balance between the OTR and the oxygen uptake rate (OUR), the latter being the product of the specific oxygen uptake rate (r_O) and the biomass concentration (X):

$$\mathrm{OUR} = r_O X \tag{5}$$

Sonnleitner and Käppeli (1986) have used a Monod type expression to calculate the specific oxygen uptake rate:

$$r_O = \frac{r_{O,\max} C}{K_O + C} \tag{6}$$

where $r_{O,\max}$ and K_O have values of 7.1×10^{-5} kg O_2 per kilogram of dry cell mass per second and $1 \times 10^{-4}\ \mathrm{kg\ m^{-3}}$, respectively. From these values, it is possible to estimate the oxygen transfer rate necessary to achieve the maximum specific oxygen uptake rate, this being of the order $12.8\ \mathrm{kg\ m^{-3}\ h^{-1}}$ (for a cell density of $50\ \mathrm{kg\ m^{-3}}$). Hence, the performance of different aeration techniques can be quantified by comparison with this maximum value.

It is generally assumed that the biomass concentration is uniform throughout the reactor. Such an approach is reasonable, as microbial cells are small (of the order 1×10^{-5} m for baker's yeast (Walker, 1998)) and of such similar density to the liquid phase that they 'follow' the liquid flow (i.e. they have a very small Stokes number). This assumption also has the advantage that it is not necessary to include an additional microbial phase in the CFD simulation in order to account for gradients in cell concentration. A biomass concentration of $50\ \mathrm{kg\ m^{-3}}$ was used in this work.

2.3. Particle tracking set-up

Another potential method for quantifying the impact of substrate gradients is to include particles which have similar flow characteristics to yeast cells and monitor the environmental conditions (i.e. sugar and oxygen concentrations) experienced by the 'cells' as a function of time using the Euler–Lagrange approach. It may be reasonably assumed that due to their size and density the representative yeast particles will have a minimal influence on the fluid flow, hence one can model the system using one-way coupling (the fluid flow influences the particle motion, but the particles do not influence the fluid flow). Using such an approach, the displacement ($\boldsymbol{x}$) of a particle is determined by integration of the particle velocity ($\boldsymbol{U}_p$):

$$\frac{d\boldsymbol{x}}{dt} = \boldsymbol{U}_p \tag{7}$$

The particle velocity is calculated by solving the particle momentum equation:

$$m_p \frac{d\boldsymbol{U}_p}{dt} = \boldsymbol{F}_p \tag{8}$$

where m_p is the mass of the particle and $\boldsymbol{F}_p$ is the sum of all forces acting upon the particle. In our model, the only inter-phase momentum transfer term considered for the particles was drag, this being calculated using the Schiller–Naumann correlation as implemented in ANSYS CFX 15.0. Turbulent dispersion of the particles was included, using the particle dispersion model as implemented in CFX, with the default value of 5 being used for the eddy viscosity ratio limit.

1000 particles were introduced into the simulation, with the injection location being a sphere with a radius of 0.01 m, located 1 m above the base of the column at the centerline. The particles were introduced over a duration of one second, commencing at $t = 240$ s.

2.4. Characterizing bioreactor performance using CFD

As previously discussed a range of techniques exist to characterize bioreactor performance. We employed a range of approaches, which can be divided into two broad categories: those based on the concentration of substrate as calculated by the CFD model, and those based on particle tracking. Table 2 summarizes the various approaches.

2.4.1. Quantifying bioreactor performance using average concentration methods

One way in which bioreactor performance can be quantified is to determine the fraction of the total volume (V) in which starvation or overflow metabolism occurs. For example, the percentage of the

reactor experiencing starvation conditions (f_S) is:

$$f_S = \frac{V_S}{V} \times 100 \tag{9}$$

where the volume of the bioreactor experiencing starvation conditions (V_S) is found by

$$V_S = \sum_{i=1}^{n} V_i \varphi_i, \quad \varphi_i = \begin{cases} 1, \bar{r}_S < m_S \\ 0, \bar{r}_S \geq m_S \end{cases} \tag{10}$$

where $\bar{r}_S$ is the average substrate uptake rate, n is the total number of cells in the computational mesh (here 35,960) and V_i is the volume of any given cell. Similarly, the percentage of the bioreactor in which overflow metabolism is occurring (f_E) can be found:

$$f_E = \frac{V_E}{V} \times 100 \tag{11}$$

where the volume of the bioreactor in which overflow metabolism is occurring (V_E) is:

$$V_E = \sum_{i=1}^{n} V_i \varphi_i, \quad \varphi_i = \begin{cases} 1, \bar{r}_S > r_{S,aero,max} \\ 0, \bar{r}_S \leq r_{S,aero,max} \end{cases} \tag{12}$$

Average rates of sugar and oxygen uptake are determined in the same manner as the instantaneous values (i.e. using Eqs. (4) and (6)), with the exception that the transient average sugar and oxygen concentrations are used instead of instantaneous concentrations. Hence, the calculated values are local with respect to volume, but are averages with respect to time.

Another option for quantifying the impact of substrate distribution on bioreactor performance using CFD is to calculate the relative yield ($Y_{relative}$). This is done by calculating the average rate of sugar consumption over the total volume and subtracting the average difference between the rate of sugar consumption and the maximum rate of aerobic sugar utilisation multiplied by the volume of the reactor where overflow metabolism occurs (V_E). This amount of sugar is assumed to be converted to biomass at the aerobic yield ($Y_{aerobic}$, 0.49 for baker's yeast) (Sonnleitner and Käppeli, 1986), while the remainder is assumed to be converted to biomass at the anaerobic yield ($Y_{anaerobic}$, 0.05 for baker's yeast) (Sonnleitner and Käppeli, 1986). Dividing this by the amount of biomass produced if all the sugar introduced (S_{Feed}) were used aerobically gives the fractional yield of the process:

$$Y_{relative} = \frac{Y_{aerobic}\left[XV\bar{r}_S - XV_E\left(\bar{r}_S - r_{S,aero,max}\right)\right] + Y_{anaerobic}XV_E\left(\bar{r}_S - r_{S,aero,max}\right)}{Y_{aerobic}S_{Feed}} \times 100 \tag{13}$$

Here it must be noted that Eq. (13) is based on the transient average conditions, and hence the time-averaged flow behaviour of the bubble column. Hence, this expression does not account for exposure of cells to fluctuating gradients. Rather than using the average conditions it is also possible to calculate the relative yield based on the instantaneous concentrations (i.e. the time averaged value ($\bar{r}_S$) is replaced by the instantaneous value r_S in Eq. (13)). Such an approach will account for the transient behaviour of the reactor.

2.4.2. Quantifying bioreactor performance using particle tracking methods

The performance of the bioreactor can be quantified using particle tracking in a range of ways. For example, it is possible to calculate the mean substrate concentration 'seen' by the particle as it travels through the reactor ($\bar{S}$):

$$\bar{S} = \frac{\int_{t=0}^{t_{sim}} S dt}{t_{sim}} \tag{14}$$

where S is the instantaneous sugar concentration 'seen' by a particle and t_{sim} is the total length of the simulation. In this instance the total simulation duration was 180 s, but we have chosen to remove the first 30 s of results (corresponding to 2–3 mixing times (McClure et al., 2015a)) in order to ensure the particles are evenly dispersed throughout the volume, thereby avoiding any possible issues with initialisation. Hence, a value of 150 s was used for t_{sim}. In practice, this integration is achieved by taking the particle track data from ANSYS CFX and then using a custom written script file in Matlab to perform the integration using the trapezoidal method.

Knowing the mean concentration of sugar 'seen' by each particle means it is possible to generate a frequency distribution of the mean (with respect to time) sugar concentrations experienced by the particles, such a distribution being generated by dividing the concentration range (0–1 kg m^{-3}) into equally sized bins (of width 0.01 kg m^{-3}) and determining the number of particles that fall into each bin. By comparing the frequency distributions for the three different sugar addition locations, it is possible to quantify the impact of the sugar introduction point on the average conditions experienced by the cells.

As previously noted, by tracking individual particles it is possible to generate a plot of the substrate (or oxygen) concentration experienced by a particle as a function of time. This can be used to determine the fraction of time each particle, for example, spends in a region of the reactor where there is a high local sugar concentration (i.e. above the maximum value for which aerobic metabolism can occur). By repeating this procedure for all particles, a histogram can be created showing the number of particles spending varying percentages of their time above the aerobic maximum sugar concentration.

An alternative method of quantifying bioreactor performance using particle tracking is to calculate the instantaneous yield (Y_t):

$$Y_t = \frac{Y}{r_S}, Y = \begin{cases} Y_{aero} r_S, r_S \leq r_{S,aero,max} \\ Y_{aero} r_{S,aero,max} + Y_{anaerobic}\left(r_S - r_{S,aero,max}\right), r_S > r_{S,aero,max} \end{cases} \tag{15}$$

From this, it is possible to calculate the average yield ($Y_{average}$) for each particle introduced into the system:

$$Y_{average} = \frac{\sum_{t=1}^{j} Y_t}{j} \tag{16}$$

where j is the total number of times at which the instantaneous yield is calculated. The integration time-step for particle tracking in ANSYS CFX differs from the simulation time step (1×10^{-3} s), and is not necessarily the same for all particles. For all of the particles examined in this work j was on average 5636. Given the relatively large number of time-steps (and hence the relatively small size of each time-step), it was felt that Eq. (16) offers a reasonable method of capturing the transient behaviour. Knowing the average instantaneous yield allows the relative yield for the population of particles to be determined:

$$Y_{relative} = \frac{1}{Y_{aerobic}}\left(\frac{\sum_{t=1}^{p} Y_{average}}{p}\right) \times 100 \tag{17}$$

where p is the total number of particles.

3. Results

3.1. Characterising bioreactor performance using average concentration methods

Fig. 3 shows the average predicted sugar concentration as a function of the addition point. As expected, introducing the sugar as a uniform source led to the situation shown in Fig. 3c, whereby there is little spatial variation in the predicted sugar concentration

and the average concentration is below the level that would lead to the production of ethanol.

In all circumstances examined, the predicted sugar concentration was on average greater than that needed for cell maintenance, meaning that no portion of the reactor was on average experiencing conditions that would lead to starvation (i.e. $f_s=0$).

In either of the more physically realistic cases (i.e. the sugar is introduced at a single point as shown in Fig. 3a and b) a local zone of high sugar concentration in the vicinity of the addition point is predicted. Such zones will lead to the production of ethanol, and it is predicted that the reactor volume experiencing over-flow metabolism (f_E) is 13% and 12% for sugar addition points 1 and 2, respectively. As previously discussed, over-flow metabolism leads to a drop in the process yield, with the extent to which this occurs being predicted using Eq. (13). Introducing the sugar at the free surface led to a yield which was 93% of the maximum, while introduction of the sugar beneath the sparger led to a predicted yield which was 75% of the maximum possible. The reason for this low yield is that below the sparger is the most poorly mixed part of the reactor, meaning that the difference between the rate of sugar uptake and the maximum aerobic rate for sugar uptake is always high in this volume. Such results may also suggest that calculating the fraction of the total reactor volume which experiences overflow metabolism (f_E) may be a poor metric, as similar values are obtained for both injection points 1 and 2, while there is a substantial difference in the predictions of relative yield for these two conditions. This difference is caused by the fact that while the relative volumes in which overflow metabolism is predicted to occur are similar, much more of the sugar introduced is diverted towards ethanol production when the addition point is below the sparger. Given that the calculation of the relative yield (Eq. (13)) takes this into account, and that the yield is the parameter of most practical interest, it is suggested that this is a better method of quantifying reactor performance.

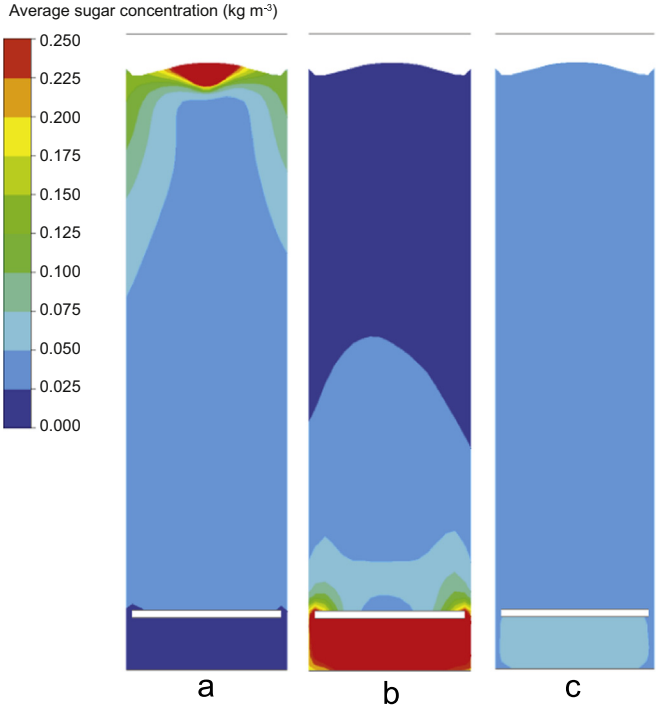

Fig. 3. Plot showing the average substrate concentration as a function of the addition location. Results are for the *XZ* plane, with substrate being introduced at the free surface (a), beneath the sparger (b), and as a uniform source (c). Overflow metabolism will occur for $S > 0.063$ kg m^{-3}.

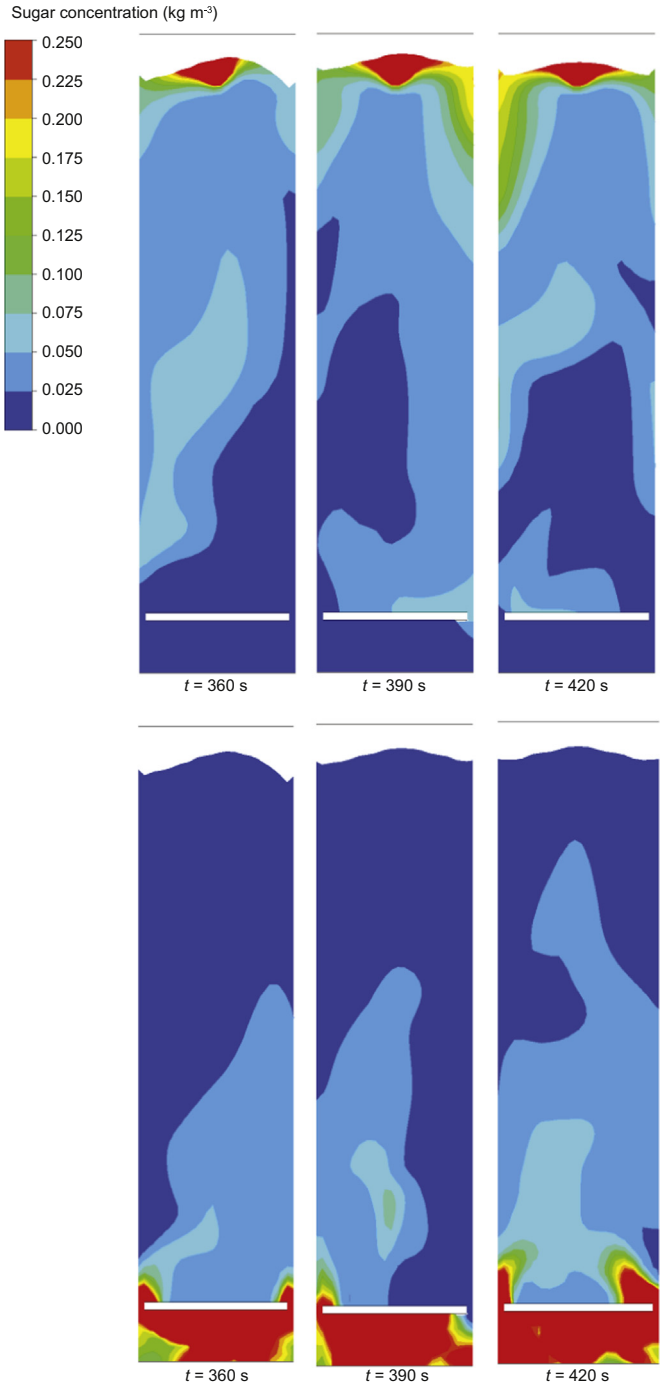

Fig. 4. Plot showing the instantaneous sugar concentration at $t=360$, 390 and 420 s. Plots on the first row are for sugar addition at the free surface, while those on the second row are for sugar addition beneath the sparger. All plots are in the *YZ* plane.

At this stage, it is worthwhile noting that the instantaneous sugar concentration varies depending on both time and location within the column; this is shown in Fig. 4, for sugar addition locations 1 (the free surface) and 2 (beneath the sparger). A plot showing the instantaneous liquid velocity field for the same time points is presented in Fig. 5. The difference between these plots also illustrates one of the key short-comings of metrics based on the average concentrations; that is, by definition they do not account for transient behaviour. Hence, they may not fully capture conditions as experienced by the cells. It must also be noted that such approaches are based on the time-averaged flow field and it

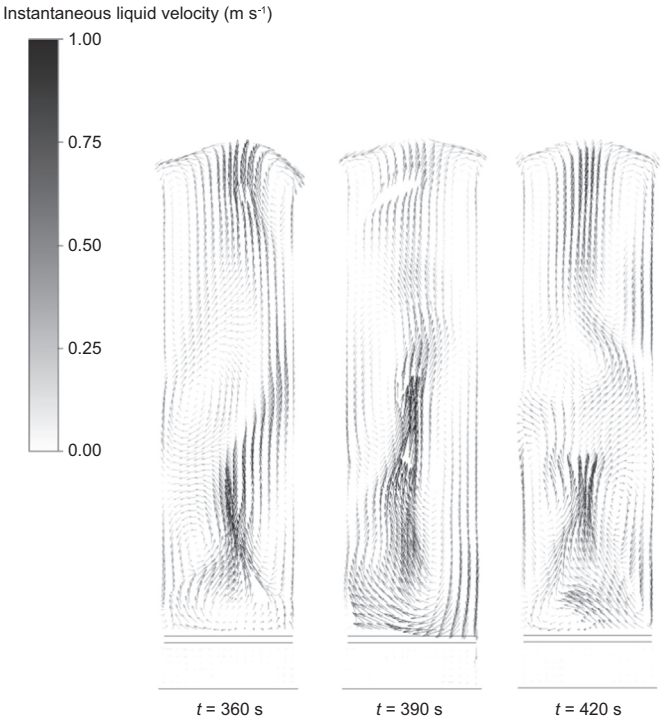

Fig. 5. Plot showing the instantaneous liquid velocity fields for $t=360$, 390 and 420 s. Plots have been made for the liquid volume only (i.e. $\alpha < 0.5$). Results are for the *XZ* plane.

is indeed possible to calculate the instantaneous yield at each time-step and from this obtain an estimate of the average yield. Performing such a calculation (using instantaneous concentrations obtained at 0.05 s intervals across the range $t=270$–420 s) and then averaging them gives relative yield values of 81% for sugar addition point 1 (the free surface) and 73% for sugar addition point two (beneath the sparger). The trend in these calculations is the same as that observed using the average results – as anticipated adding the sugar beneath the sparger is the worst location.

Calculating the yield using the instantaneous approach has two potential limitations. Firstly, this approach does not account for the duration of exposure to high substrate concentrations. If the cells are exposed to a high substrate concentration for a relatively short duration (i.e. 0.05 s) this is unlikely to have an impact upon the yield. Hence, calculation of the yield using the instantaneous values may lead to an under-estimate. Such reasoning is the most likely explanation for the fact that when the sugar is introduced at the free surface (point 1) the yield calculated based on average conditions is 93%, while it is 81% based on the instantaneous conditions. Contrastingly, the yields calculated using the instantaneous and average values for the case where the sugar is introduced beneath the sparger (point 2) are similar (75% and 73% for the average and instantaneous values, respectively). This is because the cells beneath the sparger are exposed to a zone of high substrate concentration which does not fluctuate with time (i.e. the instantaneous and average conditions are similar, as shown in Figs. 3 and 4).

A second drawback of both the instantaneous and time-averaged approaches to calculating the yield is that they do not account for the fact that the cells are transported throughout the reactor. It is felt that the best representation of the complex phenomenon inside the reactor can be achieved by accounting for both the transient concentration field as well as the motion of the cells. For this reason it may be preferable to use the more complex particle tracking type approaches which do capture information on the concentrations experienced by the cells as they move through the transient concentration field. Here it must also be noted that the predicted concentration fields are a function of both the fluid dynamics and the yeast kinetics. In our previous work we have validated the CFD model against experimental measurements of the mixing time, overall hold-up, profiles of the liquid velocity, gas velocity and profiles of the local hold-up (McClure et al., 2014c, 2015a, 2015c), hence the predictions of the flow field are expected to be reasonable. Similarly, the kinetic model used in this work was based on the experimental work of others (Sonnleitner and Käppeli, 1986). Ideally, it would be possible to have experimental data that gives the sugar concentration as a function of both time and position within the reactor. However, this is a task of some considerable experimental difficulty, and while progress has been made in the area of flow-following instrumentation for use in bioreactors (Reinecke et al., 2012), we have identified no instrument capable of monitoring the sugar concentration in the open literature. This also clearly highlights one of the advantages of a CFD model, as it gives an insight into the bioreactor performance which is difficult (or impossible) to otherwise obtain, particularly at the industrial scale.

The CFD model can also be used to predict the OTR, in this instance 3.1 kg m^{-3} h^{-1}, less than the level necessary to achieve the maximum specific oxygen consumption (12.8 kg m^{-3} h^{-1}). The model predicted an average dissolved oxygen concentration around 0.03% of saturation, which for all practical purposes can be considered as zero. This result reflects the fact that for highly aerobic cultures such as *S. cerevisiae*, the rate of oxygen uptake is essentially equal to the rate of transfer. It is also worthwhile noting that the gradients in dissolved oxygen concentration were less than those predicted for the sugar; this being a reflection of the fact that the bubbles are dispersed relatively homogenously throughout the reactor. The obvious exception to this is the volume beneath the sparger, where the model predicts that very few bubbles will be present.

Selecting the sugar concentration at which overflow metabolism will occur obviously depends on the biological model used; as previously noted, we have used a value of 0.063 kg m^{-3} which is based on the work of Sonnleitner and Käppeli (1986). This value may be somewhat conservative, as this is the value at which overflow metabolism will occur even with excess oxygen. As discussed in the previous paragraph, the rate of oxygen transfer is approximately 24% of the rate necessary to achieve the maximum specific oxygen consumption, and hence it is reasonable to think that the capacity of the cells may be limited by the availability of oxygen. If the value of the aerobic maximum uptake rate is scaled by a factor of 0.24 it was found that the predicted yield (using Eq. (13)) decreased sharply; from being in the range 75–93% to 37–41%. This decrease is clearly due to the fact that while the sugar is being introduced to the column at a rate equivalent to the maximum at which the cells can utilise it aerobically, the OTR is insufficient to realise this, which will inevitably lead to overflow metabolism. A subject of undoubted interest for any future work would be to examine the situation where the sugar addition rate is adjusted to minimise overflow metabolism (i.e. a practice that is done commercially). In the context of the current work which has the aim of evaluating different methodologies for characterising bioreactor performance it is felt that a threshold value of 0.063 kg m^{-3} is a good starting point; however, it is also acknowledged that this value will depend on the biological model used. While we have focussed on modelling aerobic production of yeast, the modelling approaches developed here can be applied more generally to processes performed in bubble column bioreactors. An issue which is likely to be key to any future applications is the development of appropriate kinetic models that are suitable for cells undergoing exposure to transient conditions (Noorman, 2011).

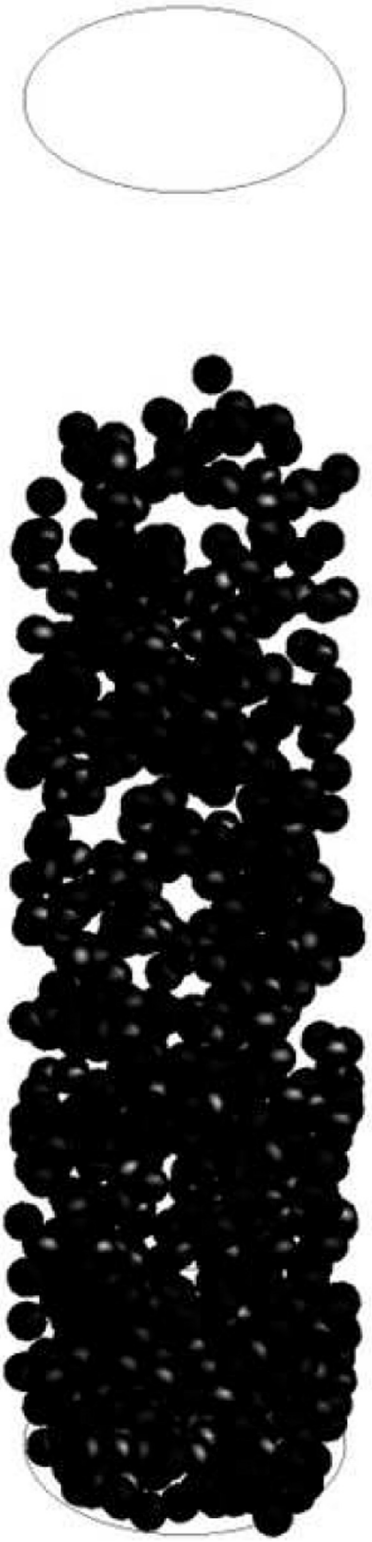

Fig. 6. Three-dimensional plot showing the location of the particles 30 s after their introduction.

3.2. Characterizing bioreactor performance using particle tracking methods

An important consideration with the particle tracking approach is ensuring that sufficient particles are introduced to cover the full reactor volume. This is important in order to obtain results which are representative, given that in reality the yeast cells will be uniformly dispersed throughout the liquid phase. With this in mind, a three-dimensional plot showing the location of the particles 30 s (i.e. 2–3 mixing times (McClure et al., 2015a)) after their introduction is given in Fig. 6. The particles are well distributed throughout the reactor; hence, it is felt that by introducing 1000 particles and waiting 30 s for them to be distributed by the fluid flow provides a reasonable representation of conditions as experienced by the yeast cells.

It is also important to ensure that the motion of the particles ensures uniform coverage of the volume; that is they start out dispersed (as shown in Fig. 6) and remain dispersed. Fig. 7 shows the location of five randomly selected particles at 1 s intervals. It can be observed that the particles remain uniformly dispersed throughout the volume, and that the particle motion is not confined to any one section of the bubble column (i.e. the particles remain uniformly dispersed).

To further quantify this, the average distance travelled by the particles was calculated, this being found to be 81 m; a distance sufficient to travel from the base of the column to the free surface approximately 54 times. Hence, it can be reasonably concluded that the particle distribution is uniform and remains this way.

As previously noted, by tracking the particles using a Lagrangian approach it is possible to generate a plot of the sugar concentrations experienced by a particle as a function of time, a representative plot being shown in Fig. 8. It can be seen that for a given particle, both the magnitude and the duration of any fluctuations in the sugar concentration depends on the injection point, illustrating the intimate relationship between the reactor design and the physiological conditions experienced by the cells. For example, introducing the sugar beneath the sparger (injection point 2) leads to the cells being exposed to zones of high concentration (i.e. above the level where ethanol production will occur) for a relatively long duration. In comparison, introducing the sugar at the free surface (injection point 1) does lead to some spikes in the sugar concentration; however, these are of relatively short duration. Introducing the sugar throughout the reactor (injection point 3) leads to a relatively uniform sugar concentration as a function of time, as would be expected. These results also illustrate an advantage of the CFD modelling approach; as such information would be very difficult to obtain experimentally.

Eqs. (15)–(17) can be used to estimate the process yield via particle tracking. Introducing the sugar uniformly led to the relative yield being 100%, a finding in agreement with the previous results (see Figs. 3 and 7), indicating that overflow metabolism does not occur under these idealised conditions. Introducing the sugar at the free surface led to the relative yield being 97% of the maximum value (0.49), suggesting that the brief exposure to a high local sugar concentration near the addition point has a small impact on the yield. Finally, introducing the sugar beneath the sparger led to the predicted yield being 0.45, or 93% of the maximum, suggesting that the greater inhomogeneity in this case has a larger impact on the predicted yield. Interestingly, the relative yields predicted by the particle tracking approach are greater than those predicted by Eq. (13) using both the average and instantaneous conditions. It is felt that calculation of the relative yield using particle tracking is preferable due to its ability to account for transient behaviour. Here it is also worthwhile noting that while the magnitude of the relative yield loss varied the trends were the same for all three metrics.

3.2.1. Characterizing performance using average particle conditions

Examining plots similar to Fig. 8 is impractical for all introduced particles; so some method of summarizing the data obtained is needed. As previously outlined, one such approach is to calculate the average sugar concentration ‘seen’ by the particles, as calculated using Eq. (14). Fig. 9 is a histogram showing the

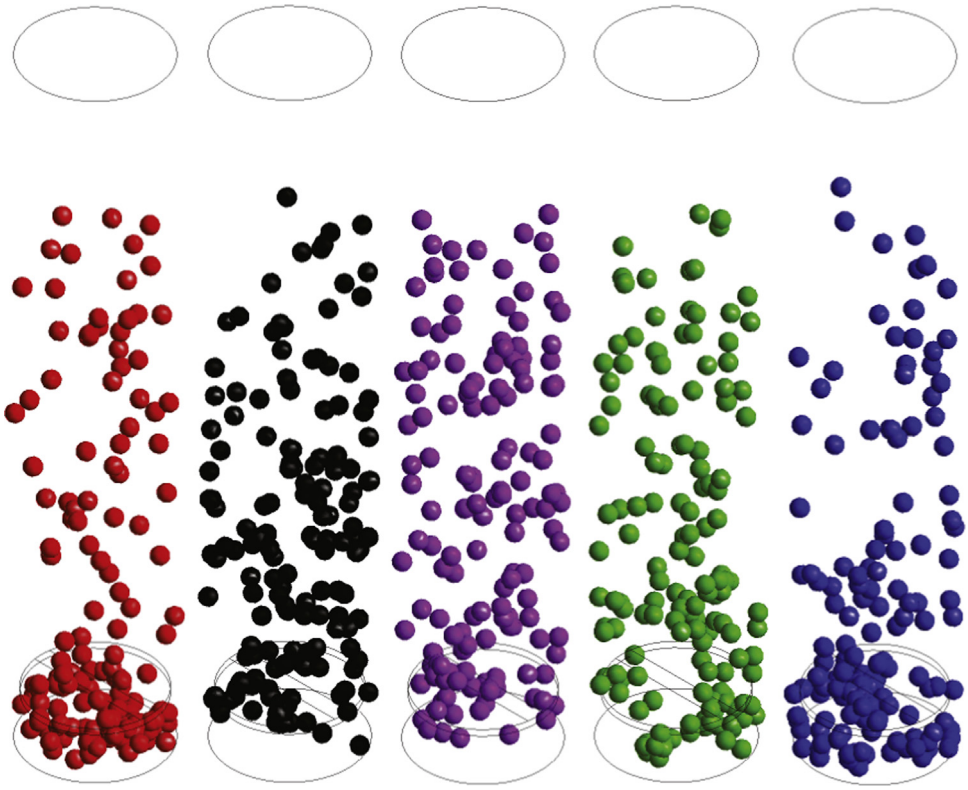

Fig. 7. Plot showing the motion of five randomly selected particles. The locations have been plotted from $t=270$ s to $t=420$ s in 1 s increments; with each dot showing the location of the particle each second.

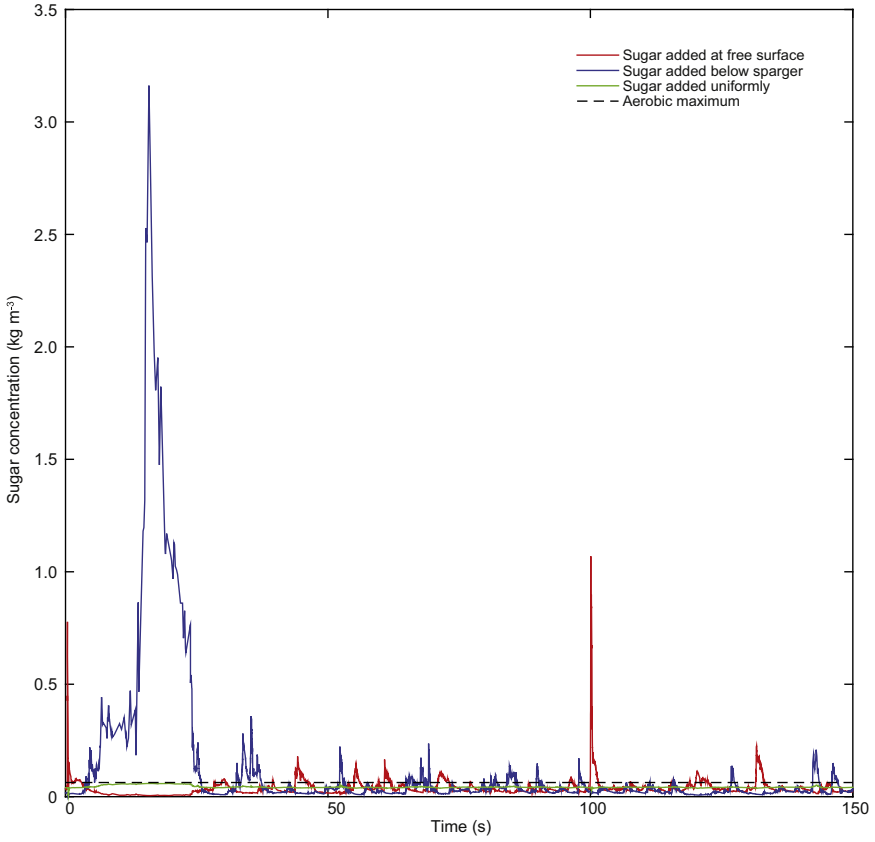

Fig. 8. Plot showing the sugar concentration experienced by a particle as a function of time for the three addition locations evaluated in this work.

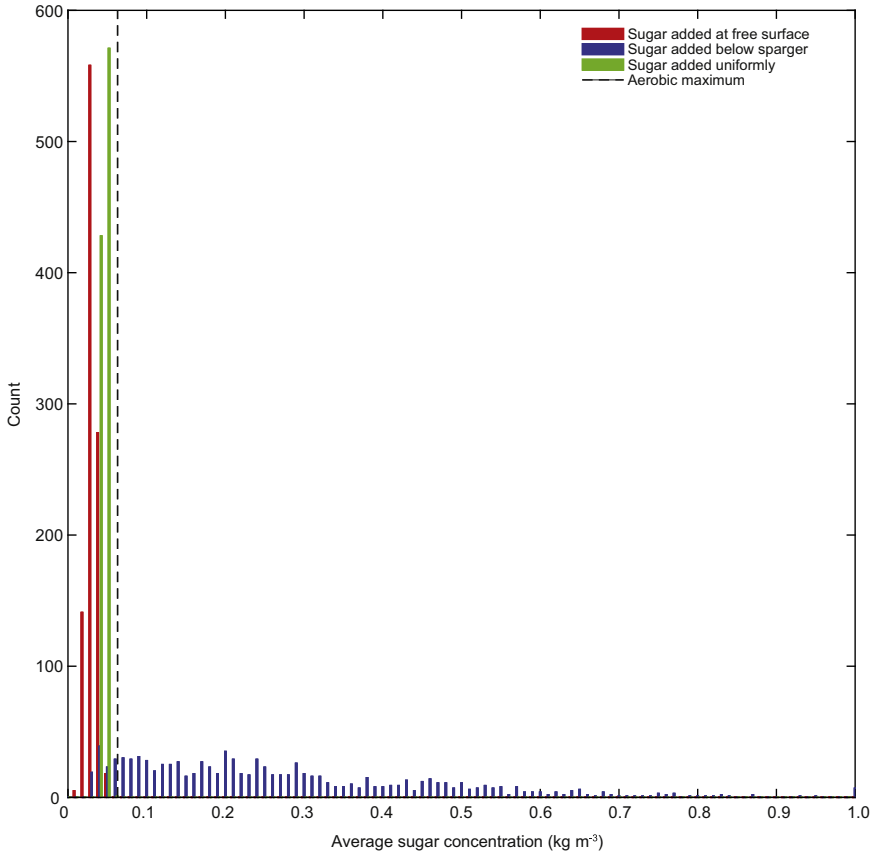

Fig. 9. Plot showing the average sugar concentrations experienced by the particles.

number of particles which experience different average sugar concentrations. Such a plot illustrates how uniform the conditions experienced by the cells are, on average. For example, the ideal situation would involve all particles on average being exposed to a sugar concentration which on average is the aerobic maximum. As shown in Fig. 9, introducing the sugar uniformly throughout the reactor closely approximates this. Adding sugar to the free surface leads to cells experiencing a slightly more diverse range of average conditions, which are still below the aerobic maximum. Contrastingly, introducing the sugar below the sparger leads to cells being exposed to a much wider range of average conditions, suggesting that significant substrate gradients are present. Results based on the average conditions experienced by the particle may be skewed towards later time periods if sugar accumulates within the bioreactor. The volume integral of the sugar concentration over the simulation domain was compared at $t=270$ s (i.e. the time when the particle tracking analysis started) and $t=420$ s (i.e. the time when the particle tracking analysis ended). It was found that the difference in the volume integrals for the three different sugar introduction points was at most 4%. Hence, it is reasonable to conclude that the results of the analysis are not skewed to any large extent by sugar accumulation within the reactor.

Such results do illustrate one of the shortcomings with this metric, in that the average result may be skewed by cells being exposed to relatively high sugar concentrations for a relatively short period of time. An alternative approach to that presented in Fig. 9 which avoids this issue is to quantify the amount of time cells spend in concentrations which are not favourable. One simple way to do this is to take the results from a plot like Fig. 8 and determine the fraction of the total time for which the particle is exposed to sugar concentrations above the aerobic maximum. By repeating this process for all particles, it is possible to generate a plot similar to Fig. 9 but which shows the number of particles which spend time above the aerobic maximum sugar concentration. Such a plot is presented in Fig. 10.

As expected (but not shown in Fig. 10) when introducing the sugar uniformly none of the particles spend any time above the aerobic maximum value, such a result being in line with results shown in Fig. 3. When the sugar is introduced beneath the sparger, particles spent more of their time being exposed to sugar concentrations above the aerobic maximum. Additionally, the range of conditions experienced by cells when the sugar was introduced beneath the sparger was wider than when it was introduced at the free surface, illustrating again that the environment experienced by the cells is less homogenous.

It is also possible to calculate the fraction of time where particles are exposed to starvation conditions (i.e. the local sugar concentration is below that needed for maintenance). It was found that particles spent practically none of their time under such a condition, a finding in line with the observations presented in Fig. 3 where the average sugar concentration was above the maintenance value.

3.2.2. *Characterizing performance by analysing oscillations*

In addition to simply calculating the average amount of time a particle spends in a zone of either high sugar concentration (leading to overflow metabolism) or low concentration (leading to starvation), it is also possible to refine the analysis to determine both the length and frequency of these oscillations. Such an insight would be of considerable interest, because exposure to such conditions for a sufficient length of time may well induce a physiological response to the environmental conditions (e.g. exposure to starvation may lead to the stress response being triggered), which in turn could lead to a drop in the yield.

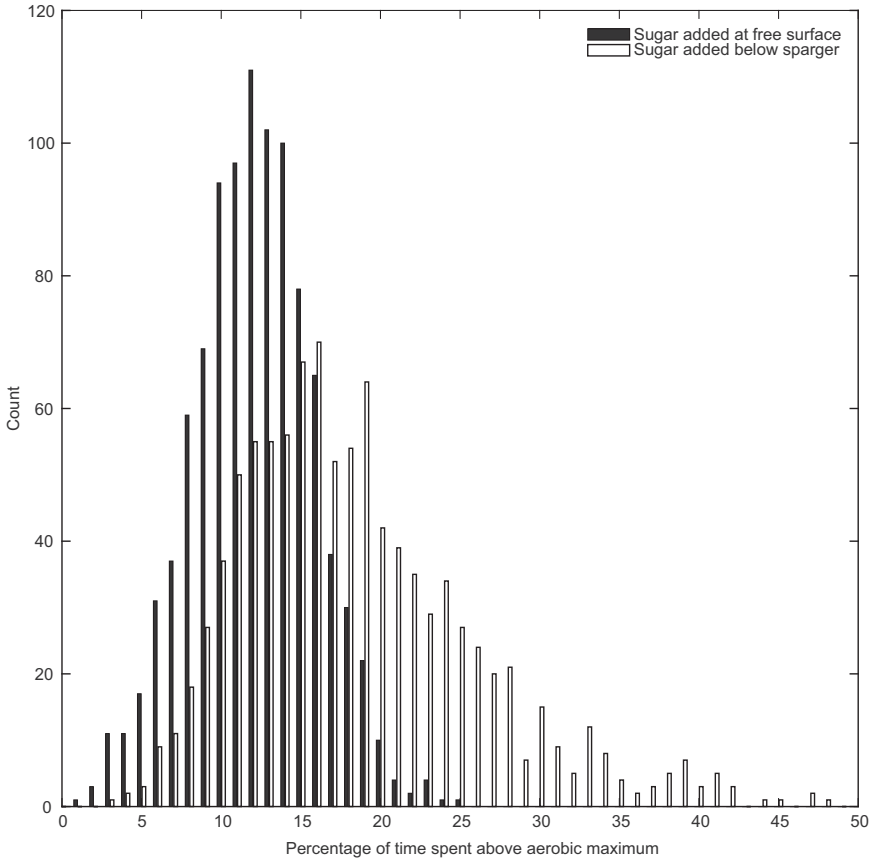

Fig. 10. Plot showing the predicted number of particles spending time above the aerobic maximum value.

As previously noted, when sugar is introduced at point 3 (i.e. uniformly throughout the reactor), the cells do not experience fluctuating conditions. However, it is instructive to compare the conditions experienced by particles when the sugar is introduced at either the free surface (point 1) or beneath the sparger (point 2).

One way to do this is to calculate the number of oscillations each particle experiences. Here, it is proposed that there are two physiologically meaningful types of oscillation, either the cell passes through a zone of high sugar concentration (above the aerobic maximum), or it passes through a zone of low sugar concentration (below that needed for cell maintenance). Fig. 11 shows the number of particles experiencing different numbers of oscillations above the aerobic maximum for each sugar addition location. Ideally, all particles would experience no oscillations above the aerobic maximum value, such behaviour being observed when the sugar is introduced uniformly. It may be reasonably concluded that the more oscillations the cells experience, the less uniform conditions in the bioreactor are; such behaviour is shown in Fig. 11, where introduction of the sugar beneath the sparger leads to cells on average experiencing more oscillations than when the sugar is introduced at the free surface.

It is also possible to generate a plot similar to Fig. 11 showing the number of times particles experience starvation conditions. However, it was found (in line with previous results), that the particles generally did not experience such conditions.

Fig. 8 shows that the oscillations experienced by the particle can vary in duration. One of the shortcomings of simply counting the number of oscillations is that it does not take into account the length of the oscillation. This aspect may well be important, because if a cell experiences an oscillation with a similar time-scale to that of the fluid flow (of the order 1×10^{-3} s), it is unlikely that this will have any impact. However, if a cell experiences an oscillation of longer duration (i.e. of the order 30 s) this may be of physiological relevance (Lara et al., 2006). One way to quantify this behaviour is to discretise the predicted range of oscillation lengths and determine the number of times each length occurs for the entire particle population. Here, we have used oscillation lengths ranging from 0–60 s, using 1 s increments. It can be appreciated however; that plotting the number of oscillations in this instance is unlikely to give a reasonable representation of the behaviour, as this will favour oscillations of small duration. Hence, we have weighted the count by the relative length of the oscillation (i.e. the oscillation duration divided by the length of the simulation, here 150 s). From this, the relative frequency is calculated, with results being presented in Fig. 12.

When the sugar was introduced at the free surface, particles tended to experience oscillations of relatively short duration, such behaviour arising from the fact that they are being transported quickly through the zone of high sugar concentration near the addition point. Given the relatively short duration of these oscillations it is unlikely that exposure to fluctuations on this time-scale would have a significant physiological impact upon the yeast cells.

Contrastingly, when the sugar is introduced beneath the sparger, it is possible for some particles to experience oscillations of more than 30 s in duration, which as previously noted (Lara et al., 2006) may be of physiological relevance. Introducing the sugar here leads to the cells experiencing much more varied conditions (as quantified by oscillation lengths), a result in line with those presented in Fig. 11. Given that the length of these oscillations is of physiological relevance an interesting area for future work would be to include a more complex model of yeast biology, for example using the approach outlined by Lapin et al. (2006).

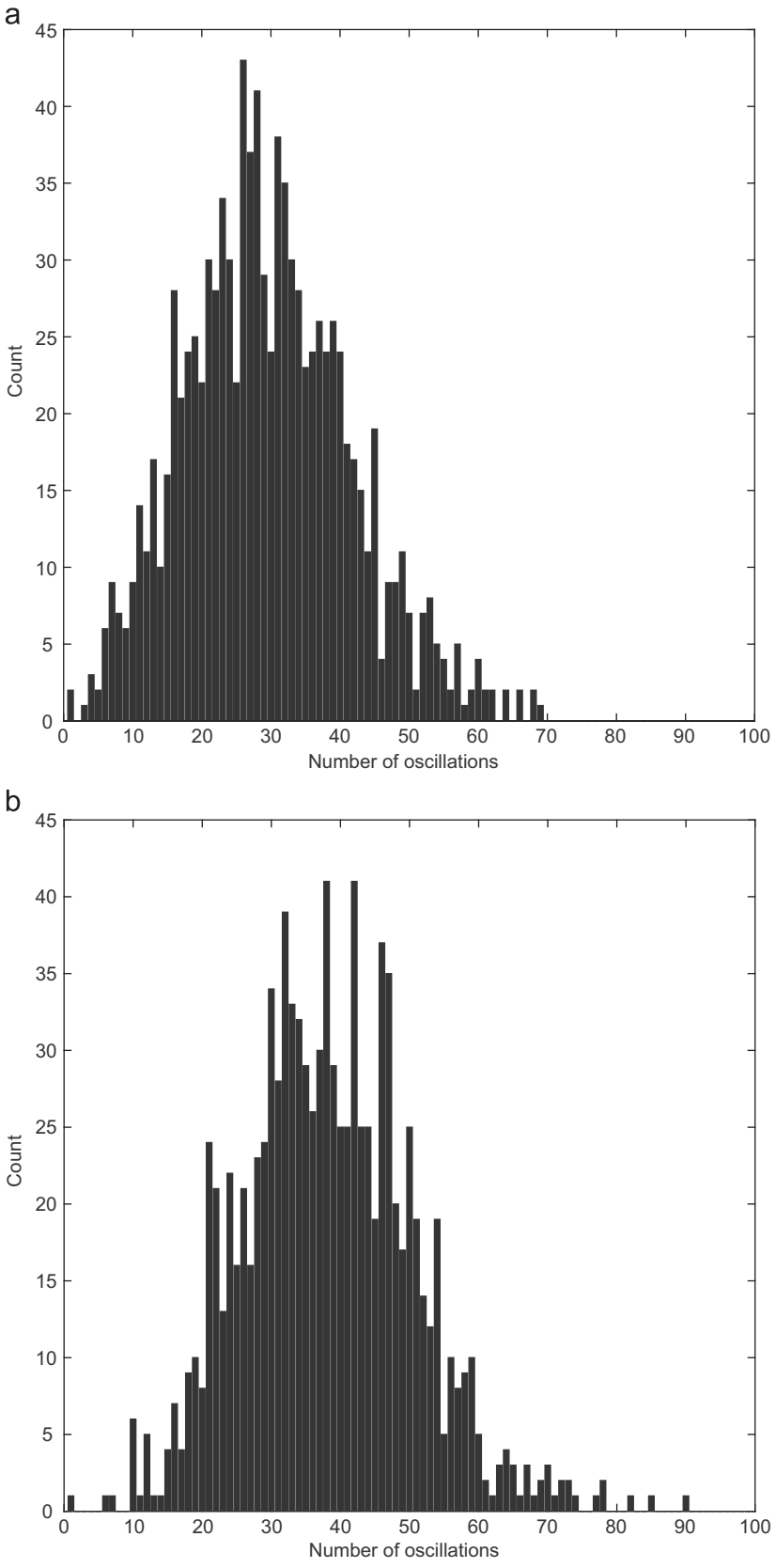

Fig. 11. Histograms showing the number of oscillations above the aerobic maximum sugar concentration for addition point 1 (a) or point 2 (b). Here 1000 particles in total have been added.

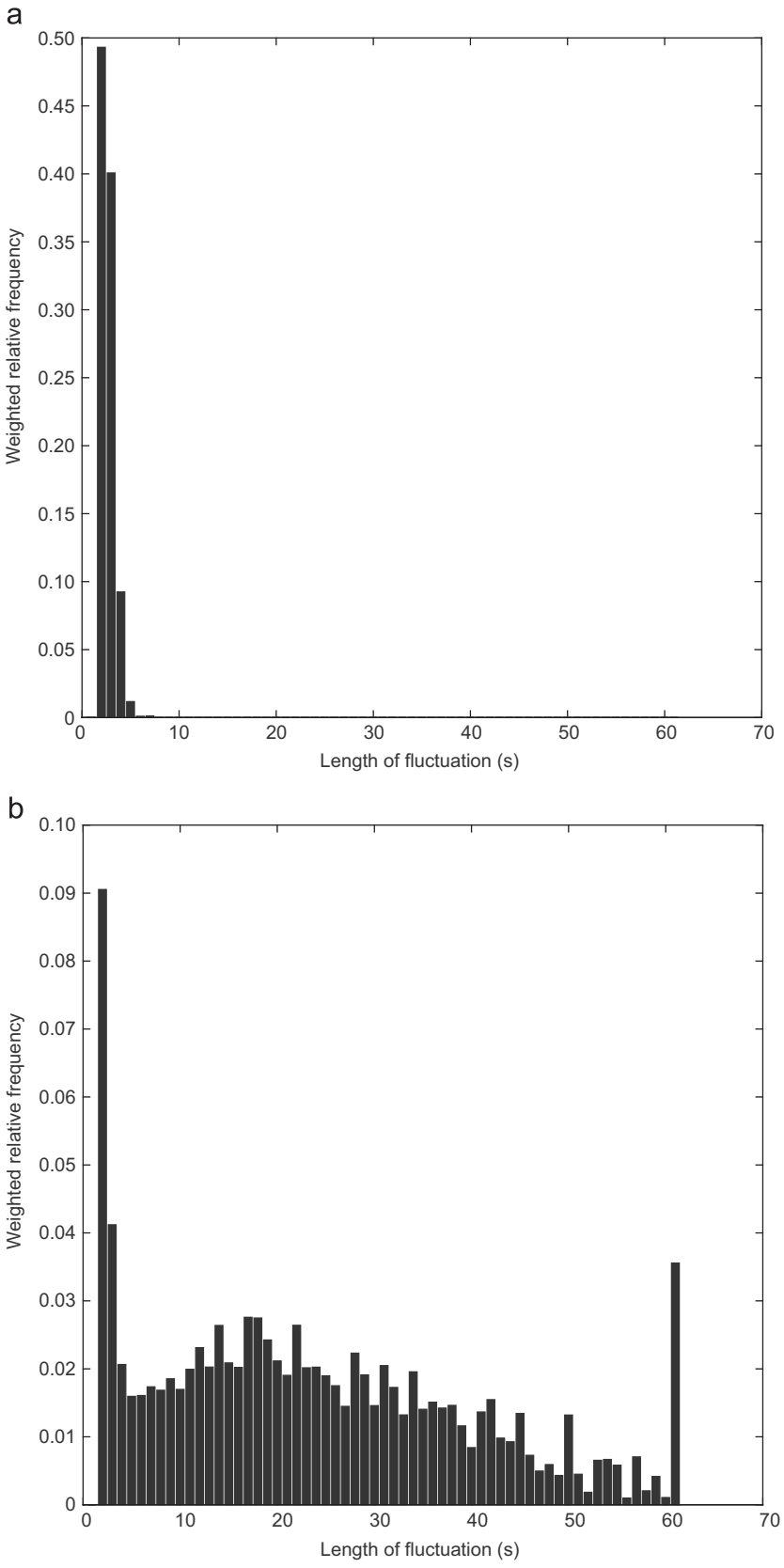

Fig. 12. Histograms showing the weighted relative frequency of the length of oscillations above the aerobic maximum sugar concentration. Results are presented for the introduction of sugar at the free surface (a) and below the sparger (b).

Table 3
Comparison of results using the different metrics evaluated in this work.

	Method	Results	Comments
Concentration Based Methods	Calculate volume of reactor experiencing overflow metabolism. Eqs. (11) and (12).	13 and 12% for sugar introduction at the free surface and beneath the sparger, respectively.	Metric may not be meaningful as it does not account for the amount of sugar consumed anaerobically.
	Calculate volume of reactor experiencing starvation. Eqs. (9) and (10).	Starvation not predicted.	
	Calculate average relative yield. Eq. (13).	93% and 75% for sugar introduction at the free surface and beneath the sparger, respectively.	Simple, relevant metric. May overestimate yield loss by not accounting for transient behaviour.
	Calculate instantaneous relative yield. Eq. (13).	81% and 73 for sugar introduction at the free surface and beneath the sparger, respectively.	Simple, relevant metric. May overestimate yield loss by not accounting for duration of transients or particle motion.
Particle Tracking Methods	Generate plot of substrate concentration as a function of time for each particle. (e.g. Fig. 8).	Clearly illustrates transient behaviour.	Impractical for any reasonable number of particles.
	Calculate average yield for each particle Eqs. (15)–(17).	97% and 93% for sugar introduction at the free surface and beneath the sparger, respectively.	Relevant metric, accounts for transient behaviour.
	Calculate frequency distribution of mean sugar concentration Eq. (14).	Introducing sugar beneath sparger leads to much less homogenous conditions.	Relatively simple metric that summarizes the degree of inhomogeneity.
	Calculate amount of time spent in overflow or starvation conditions.	Introducing sugar beneath sparger leads to much less homogenous conditions.	Relatively simple metric that summarizes the degree of inhomogeneity.
	Calculate the number, length or frequency at which particles experience oscillations above the aerobic maximum or below the maintenance value.	Oscillations occur with greater frequency and length when sugar is introduced beneath the sparger.	Method gives an insight into the fluctuating conditions experienced by the cells.

For ease of comparison, a summary of the various methods used to quantify bioreactor performance evaluated in this work are presented in Table 3.

4. Conclusions

In this work we examined the issue of characterizing the performance of a bioreactor using a previously validated (against very extensive experimental data) CFD model. This was done by simulating the addition of substrate at three different locations; various metrics were then proposed to evaluate the impact of the substrate addition location on the bioreactor performance.

Of the methods examined, it was found that quantifying bioreactor performance by calculating the volume experiencing overflow metabolism was not a particularly useful approach. Contrastingly, calculating the relative yield by using the average sugar concentrations, using the instantaneous sugar concentrations or averaging the instantaneous results from the particle tracking approach is felt to be a more useful performance metric. Of the three methods of determining the relative yield, the method based on the particle tracking approach is likely to be the more suitable as it fully accounts for transient behaviour.

We have also shown how particle tracking can be used to determine the number, duration and frequency with which cells experience oscillations in sugar concentration. This information has obvious physiological relevance, and can be used to characterize the degree of inhomogeneity in the reactor. Furthermore, the approach could be readily extended to other relevant operational parameters (e.g. local variations in shear stress, oxygen concentration, temperature, and pH).

Overall, it is clear that the location of the substrate introduction point is a key parameter in the design and operation of a bioreactor. Furthermore, it is equally clear that the use of CFD has tremendous potential in both quantifying the complex, highly transient behaviour occurring inside industrial bubble column bioreactors as well as identifying meaningful metrics with which the design and performance of such reactors can be optimised. Key areas currently being researched include examining the impact of reactor scale on performance and quantifying the value of the performance metrics examined in this paper for other industrially relevant microorganisms.

Nomenclature

Symbol	Description, Units
a	interfacial area for mass transfer, m^{-1}
C	dissolved oxygen concentration, kg m^{-3}
C_1	constant in k–ε model (–)
C_2	constant in k–ε model (–)
C_D	bubble drag coefficient (–)
$C_{D,\infty}$	drag coefficient of isolated bubble (–)
C_μ	constant in k–ε model (–)
C^*	saturation oxygen concentration, kg m^{-3}
D_L^{φ}	kinematic diffusivity, m^2 s^{-1}
d_b	bubble diameter, m
$\boldsymbol{F}_D$	drag force acting on bubble, kg m^{-2} s^{-2}
$\boldsymbol{F}_p$	forces acting on particle, kg m s^{-2}
$f(\alpha_G)$	volume fraction correction term (–)
f_E	fraction of total reactor volume experiencing overflow metabolism (–)
f_S	fraction of total reactor volume experiencing starvation conditions (–)
H	Henry's Law constant, Pa m^3 mol^{-1}
i	number of mesh cells (–)
j	number of time steps (–)
k	turbulence kinetic energy, m^2 s^{-2}
k_L	liquid film mass transfer coefficient, m/s
k_S	surfactant constant (–)
K_O	oxygen saturation parameter, kg m^{-3}
K_S	substrate saturation parameter, kg m^{-3}

m_p particle mass, kg
m_S maintenance coefficient, s^{-1}
$\boldsymbol{M}_{LG}$ inter-phase momentum transfer, kg m^{-2} s^{-2}
n number of cells in computational mesh (–)
OTR oxygen transfer rate, kg m^{-3} s^{-1}
OUR oxygen uptake rate, kg m^{-3} s^{-1}
p number of particles (–)
P_L Production of turbulence by shear in the liquid phase, kg m^{-1} s^{-3}
r_O oxygen uptake rate, s^{-1}
$r_{O,\max}$ maximum specific oxygen uptake rate, s^{-1}
r_S sugar uptake rate, s^{-1}
$\bar{r}_S$ transient average sugar uptake rate, s^{-1}
$r_{S,\max}$ maximum specific substrate uptake rate, s^{-1}
$r_{S,aero,\max}$ maximum aerobic sugar consumption rate, s^{-1}
S substrate concentration, kg m^{-3}
$\bar{S}$ average substrate concentration, kg m^{-3}
S_{Feed} sugar feed rate, kg s^{-1}
S_G source term for gas phase, kg m^{-3} s^{-1}
S_L^{φ} source term for sugar, kg m^{-3} s^{-1}
$Sc_{t,L}$ turbulent Schmidt number, dimensionless
t time, s
t_{sim} simulation duration, s
$T_{LG,\varepsilon}$ inter-phase transfer term for ε, kg m^{-1} s^{-4}
$T_{LG,k}$ inter-phase transfer term for k, kg m^{-1} s^{-3}
$\boldsymbol{U}_G$ gas velocity, m s^{-1}
$\boldsymbol{U}_L$ liquid velocity, m s^{-1}
$\boldsymbol{U}_p$ particle velocity, m s^{-1}
V volume, m^{-3}
V_E volume of reactor experiencing overflow metabolism, m^{-3}
V_i volume of cell i, m^{-3}
V_S volume of reactor experiencing starvation conditions, m^{-3}
x distance in x direction, m
$\boldsymbol{x}$ particle displacement, m
X cell concentration, kg m^{-3}
y distance in y direction, m
Y yield, dimensionless
$Y_{aerobic}$ biomass yield under aerobic conditions (–)
$Y_{anaerobic}$ biomass yield under anaerobic conditions (–)
$Y_{average}$ average yield, dimensionless
Y_{O2} mass fraction of oxygen, dimensionless
$Y_{relative}$ relative yield, dimensionless
Y_t instantaneous yield at time t, dimensionless
z distance in z direction, m
α volume fraction of gas phase, dimensionless
ε turbulence energy dissipation rate, m^2 s^{-3}
μ dynamic viscosity, kg m^{-1} s^{-1}
$\mu_{t,L}$ turbulent viscosity, kg m^{-1} s^{-1}
ρ density, kg m^{-3}
σ_ε constant in k–ε model, dimensionless
σ_k constant in k-ε model, dimensionless
φ mass fraction of scalar (sugar), dimensionless
Γ inter-phase mass transfer rate, kg m^{-3} s^{-1}

Acknowledgements

The authors gratefully acknowledge that this work was partially funded by ARC Linkage Grant LP120100608. The authors would also like to acknowledge funding from the ARC Training Centre for the Australian Food Processing Industry in the 21st Century (IC140100026).

Appendix A

Here, we briefly describe the equations used by the CFD model in this work. Conservation of mass, momentum and species (i.e. oxygen) for the gas phase are calculated using:

$$\frac{\partial(\rho_G\alpha_G)}{\partial t}+\nabla\bullet(\rho_G\alpha_G\boldsymbol{U}_G)=S_G \quad (A-1)$$

$$\frac{\partial(\rho_G\alpha_G)}{\partial t}+\nabla\bullet(\rho_G\alpha_G\boldsymbol{U}_G\otimes\boldsymbol{U}_G)=-\alpha_G\nabla p+\nabla\bullet\left(\alpha_G\mu_{G,\text{eff}}\left[\nabla\boldsymbol{U}_G+(\nabla\boldsymbol{U}_G)^T-\frac{2}{3}\boldsymbol{\delta}\nabla.\boldsymbol{U}_G\right]\right)+\alpha_G\rho_G\boldsymbol{g}+\boldsymbol{M}_{GL} \quad (A-2)$$

$$\frac{\partial(\rho_G\alpha_G Y_{O2})}{\partial t}+\nabla\bullet(\alpha_G(\rho_G\boldsymbol{U}_G-\rho_G D_{\text{eff},O2}\nabla Y_{O2}))=S_G-\Gamma_{GL} \quad (A-3)$$

Conservation equations for the liquid phase are of the same form, with the exception that the liquid velocity, volume fraction and density are used. Similarly, the mass fraction of oxygen (Y_{O2}) becomes the mass fraction of dissolved oxygen.

The inter-phase momentum transfer term in Eq. (A-2) ($\boldsymbol{M}_{GL}$) was modelled as the sum of contributions arising from drag and turbulent dispersion. The drag force per volume for spherical bubbles ($\boldsymbol{F}_D$) is calculated according to:

$$\boldsymbol{F}_D=\frac{3}{4}\frac{C_D}{d_b}\rho_L\alpha_G(\boldsymbol{U}_G-\boldsymbol{U}_L)|\boldsymbol{U}_G-\boldsymbol{U}_L| \quad (A-4)$$

where C_D is the drag coefficient. Here, this has been split into three components; the drag coefficient of an isolated bubble ($C_{D,\infty}$); a volume fraction correction term ($f(\alpha)$) that accounts for the presence of other bubbles, and a surfactant constant (k_s) that accounts for the effect of compounds in the liquid phase on the bubble drag:

$$C_D=C_{D,\infty}k_s f(\alpha_G) \quad (A-5)$$

where the drag coefficient of an isolated bubble was calculated using the correlation of Grace et al. (Clift et al., 1978). A value of 2 was used for the surfactant constant (k_s), based on our previous experimental work (McClure et al., 2014a) and associated modelling (McClure et al., 2015c). A modified form of the volume fraction correction term developed by Simonnet et al. (Simonnet et al., 2007) was used here, whereby there is no hindered rise. Hence, $f(\alpha)$ was calculated thusly:

$$f(\alpha_G)=\begin{cases}\min(f'(\alpha_G),1.0) & f'(\alpha_G)>1\\ f'(\alpha_G) & f'(\alpha_G)\le 1\end{cases} \quad (A-6)$$

$$f'(\alpha_G)=(1-\alpha_G)\left[(1-\alpha_G)^{25}+\left(4.8\frac{\alpha_G}{1-\alpha_G}\right)^{25}\right]^{-\frac{2}{25}} \quad (A-7)$$

Turbulent dispersion was modelled using the Favre-averaged drag formulation developed by Burns et al. (2004) as implemented in ANSYS CFX:

$$\boldsymbol{F}_{TD}=\boldsymbol{M}_{GL,Drag}\frac{\upsilon_{T,L}}{Sc_{t,L}}\left(\frac{\nabla\alpha_G}{\alpha_G}-\frac{\nabla\alpha_L}{\alpha_L}\right) \quad (A-8)$$

$\boldsymbol{M}_{GL,Drag}$ is the inter-phase momentum transfer due to drag, while $Sc_{t,L}$ is the turbulent Schmidt number for the liquid phase; this has the default value (0.9).

As previously noted, the k–ε model was used to account for turbulence in the liquid phase. The transport equations for turbulence kinetic energy (k) and the turbulence kinetic energy dissipation rate (ε) for the liquid phase are:

$$\frac{\partial(\alpha_L\rho_L k_L)}{\partial t}+\nabla\bullet\left(\alpha_L\left(\rho_L k_L\boldsymbol{U}_L-\left(\mu+\frac{\mu_{t,L}}{\sigma_k}\right)\nabla k_L\right)\right)=\alpha_L(P_L-\rho_L\varepsilon_L)+T_{LG,k} \quad (A-9)$$

$$\frac{\partial(\alpha_L\rho_L\varepsilon_L)}{\partial t}+\nabla\bullet\left(\alpha_L\rho_L\varepsilon_L\boldsymbol{U}_L-\left(\mu+\frac{\mu_{t,L}}{\sigma_\varepsilon}\right)\nabla\varepsilon_L\right)$$
$$=\alpha_L\frac{\varepsilon_L}{k_L}(C_1P_L-C_2\rho_L\varepsilon_L)+T_{LG,\varepsilon} \quad (A-10)$$

Standard values were used for the model constants C_1, C_2, σ_k and σ_ε, the values being 1.44, 1.92, 1.0 and 1.3, respectively. $\mu_{t,L}$ is the turbulent viscosity and was calculated thusly:

$$\mu_{t,L}=C_\mu\rho_L\left(\frac{k_L^2}{\varepsilon_L}\right) \quad (A-11)$$

where C_μ was set to 0.09. $T_{LG,k}$ and $T_{LG,\varepsilon}$ are source terms that account for bubble-induced turbulence. Here,, we have used the model developed by Pfleger and Becker (2001), where the source terms are:

$$T_{LG,k}=\alpha_L C_1|\boldsymbol{M}_{LG}||\boldsymbol{U}_G-\boldsymbol{U}_L| \quad (A-12)$$

$$T_{LG,\varepsilon}=\frac{\varepsilon}{k}\alpha_L C_1|\boldsymbol{M}_{LG}||\boldsymbol{U}_G-\boldsymbol{U}_L| \quad (A-13)$$

When implementing the turbulence source terms only interphase momentum transfer due to drag was included.

The transport of sugar throughout the liquid was modelled using the equation describing a generic scalar transported by the fluid flow:

$$\frac{\partial(\alpha_L\rho_L\varphi_L)}{\partial t}+\nabla\bullet(\alpha_L\rho_L\boldsymbol{U}_L\varphi_L)-\nabla\bullet\left(\alpha_L\left(\rho_L D_L^{\varphi}+\frac{\mu_{t,L}}{Sc_{t,L}}\right)\nabla\varphi\right)=S_L^{\varphi} \quad (A-14)$$

where φ_L is the mass fraction of sugar and D_L^{φ} is the kinematic diffusivity of the sugar in the liquid. Here, we assumed that advection is the dominant mechanism of sugar transport; hence the laminar kinematic diffusivity has been set to zero. S_L^{φ} is a source term; this corresponds to the introduction of sugar into the bubble column. Again, the default value for the turbulent Schmidt number (0.9) has been used.

References

Auling, G., Bellgardt, K.H., Diekmann, H., Thoma, M., 1984. Dynamics of growth in batch and continuous cultures of *Saccharomyces cerevisiae*; during shifts from aerobiosis to anaerobiosis and reverse. Appl. Microbiol. Biotechnol. 19, 353–357.

Blanch, H.W., Clark, D.S., 1997. Biochemical Engineering. CRC Press, Boca Raton.

Braun, M., 2012. Multiphase Flow Modelling. ANSYS Inc.

Burns, A.D., Frank, T., Hamill, I., Shi, J.-M., 2004. The favre averaged drag model for turbulent dispersion in eulerian multi-phase flows. In: Proceedings of the 5th International Conference on Multiphase Flow, Yokohama, Japan.

Bylund, F., Guillard, F., Enfors, S.O., Trägårdh, C., Larsson, G., 1999. Scale down of recombinant protein production: a comparative study of scaling performance. Bioprocess Biosyst. Eng. 20, 377–389.

Clift, R., Grace, J.R., Weber, M.E., 1978. Bubbles, Drops and Particles. Academic Press, New York.

Doran, P., 1995. Bioprocess Engineering Principles. Elsevier, Oxford.

Enfors, S.O., Jahic, M., Rozkov, A., Xu, B., Hecker, M., Jürgen, B., Krüger, E., Schweder, T., Hamer, G., O'Beirne, D., Noisommit-Rizzi, N., Reuss, M., Boone, L., Hewitt, C., McFarlane, C., Nienow, A., Kovacs, T., Trägårdh, C., Fuchs, L., Revstedt, J., Friberg, P.C., Hjertager, B., Blomsten, G., Skogman, H., Hjort, S., Hoeks, F., Lin, H.Y., Neubauer, P., van der Lans, R., Luyben, K., Vrabel, P., Manelius, Å., 2001. Physiological responses to mixing in large scale bioreactors. J. Biotechnol. 85, 175–185.

George, S., Larsson, G., Olsson, K., Enfors, S.O., 1998. Comparison of the Baker's yeast process performance in laboratory and production scale. Bioprocess Biosyst. Eng. 18, 135–142.

Hewitt, C.J., Nienow, A.W., 2007. The scale-up of microbial batch and fed-batch fermentation processes. In: Allen, I., Laskin, S.S., Geoffrey, M.G. (Eds.), Advances in Applied Microbiology. Academic Press, Amsterdam, pp. 105–135.

Kantarci, N., Borak, F., Ulgen, K.O., 2005. Bubble column reactors. Process Biochem. 40, 2263–2283.

Kavanagh, J.M., Barton, G.W., 2008. Productivity improvement of recombinant *Escherichia coli* fermentation via robust optimization. Bioprocess Biosyst. Eng. 31, 137–143.

Lapin, A., Schmid, J., Reuss, M., 2006. Modeling the dynamics of *E. coli* populations in the three-dimensional turbulent field of a stirred-tank bioreactor – a structured-segregated approach. Chem. Eng. Sci. 61, 4783–4797.

Lara, A.R., Galindo, E., Octavio, R.T., Palomares, L.A., 2006. Living with heterogeneities in bioreactors: understanding the effects of environmental gradients on cells. Mol. Biotechnol. 34, 355.

McClure, D.D., Aboudha, N., Kavanagh, J.M., Fletcher, D.F., Barton, G.W., 2015a. Mixing in bubble column reactors: experimental study and CFD modeling. Chem. Eng. J. 264, 291–301.

McClure, D.D., Deligny, J., Kavanagh, J.M., Fletcher, D.F., Barton, G.W., 2014a. Impact of surfactant chemistry on bubble column systems. Chem. Eng. Technol. 37, 652–658.

McClure, D.D., Kavanagh, J.M., Fletcher, D.F., Barton, G.W., 2013. Development of a CFD Model of bubble column bioreactors: Part one – a detailed experimental study. Chem. Eng. Technol. 36, 2065–2070.

McClure, D.D., Kavanagh, J.M., Fletcher, D.F., Barton, G.W., 2014b. Development of a CFD model of bubble column bioreactors: Part two – comparison of experimental data and CFD predictions. Chem. Eng. Technol. 37, 131–140.

McClure, D.D., Lee, A.C., Kavanagh, J.M., Fletcher, D.F., Barton, G.W., 2015b. Impact of surfactant addition on oxygen mass transfer in a bubble column. Chem. Eng. Technol. 38, 1–10.

McClure, D.D., Norris, H., Kavanagh, J.M., Fletcher, D.F., Barton, G.W., 2014c. Validation of a computationally efficient computational fluid dynamics (CFD) model for industrial bubble column bioreactors. Ind. Eng. Chem. Res. 53, 14526–14543.

McClure, D.D., Norris, H., Kavanagh, J.M., Fletcher, D.F., Barton, G.W., 2015c. Towards a CFD model of bubble columns containing significant surfactant levels. Chem. Eng. Sci. 127, 189–201.

Morchain, J., Gabelle, J.-C., Cockx, A., 2014. A coupled population balance model and CFD approach for the simulation of mixing issues in lab-scale and industrial bioreactors. AIChE J. 60, 27–40.

Neubauer, P., Junne, S., 2010. Scale-down simulators for metabolic analysis of large-scale bioprocesses. Curr. Opin. Biotechnol. 21, 114–121.

Noorman, H., 2011. An industrial perspective on bioreactor scale-down: what we can learn from combined large-scale bioprocess and model fluid studies. Biotechnol. J. 6, 934–943.

Pfleger, D., Becker, S., 2001. Modelling and simulation of the dynamic flow behaviour in a bubble column. Chem. Eng. Sci. 56, 1737–1747.

Pham, H.T.B., Larsson, G., Enfors, S.-O., 1998. Growth and energy metabolism in aerobic fed-batch cultures of Saccharomyces cerevisiae: simulation and model verification. Biotechnol. Bioeng. 60, 474–482.

Postma, E., Alexander Scheffers, W., Van Dijken, J.P., 1989. Kinetics of growth and glucose transport in glucose-limited chemostat cultures of Saccharomyces cerevisiae CBS 8066. Yeast 5, 159–165.

Reinecke, S., Deutschmann, A., Jobst, K., Kryk, H., Friedrich, E., Hampel, U., 2012. Flow following sensor particles—validation and macro-mixing analysis in a stirred fermentation vessel with a highly viscous substrate. Biochem. Eng. J. 69, 159–171.

Simonnet, M., Gentric, C., Olmos, E., Midoux, N., 2007. Experimental determination of the drag coefficient in a swarm of bubbles. Chem. Eng. Sci. 62, 858–866.

Sonnleitner, B., Käppeli, O., 1986. Growth of Saccharomyces cerevisiae is controlled by its limited respiratory capacity: formulation and verification of a hypothesis. Biotechnol. Bioeng. 28, 927–937.

Sweere, A.P.J., Matla, Y.A., Zandvliet, J., Luyben, K.C.A.M., Kossen, N.W.F., 1988. Experimental simulation of glucose fluctuations. Appl. Microbiol. Biotechnol. 28, 109–115.

Vetter, A., 2009. Sequential Co-simulation as Method to Couple CFD and Biological Growth in a Yeast Reactor. FIT-Verlag, Paderborn.

Vrábel, P., van der Lans, R.G.J.M., van der Schot, F.N., Luyben, K.C.A.M., Xu, B., Enfors, S.-O., 2001. CMA: integration of fluid dynamics and microbial kinetics in modelling of large-scale fermentations. Chem. Eng. J. 84, 463–474.

Walker, G.M., 1998. Yeast Physiology and Biotechnology. J. Wiley & Sons, Chichester; New York.

Xu, B., Jahic, M., Blomsten, G., Enfors, S.O., 1999. Glucose overflow metabolism and mixed-acid fermentation in aerobic large-scale fed-batch processes with *Escherichia coli*. Appl. Microbiol. Biotechnol. 51, 564–571.